Viscoelastic Creep Behavior of Filament-Wound Case Materials

S.W. Beckwith*
Hercules, Magna, Utah

The viscoelastic creep behavior of an S-901 glass/epoxy composite used in a solid rocket motor case is examined for a variety of loading conditions. Samples were removed from the forward dome region of a filament-wound motor case at fiber angles of ±20 and ±70 deg. They were tested at several stress levels in tension and four-point beam bending to determine the creep response through several creep-recovery cycles. Constant displacement rate tests also were conducted using the four-point beam bending test to evaluate hysteresis at relatively low stress levels. The behavior was found to be similar in many ways to that previously found for autoclaved, flat-plate samples tested at equivalent conditions. The creep behavior was found to follow a power law in time, $D = D_0 + D_1 t^n$, where D is the creep compliance (psi^{-1}), D_0 is the initial elastic compliance, and D_1 and n define the viscoelastic response characteristics. In the linear viscoelastic range, $n = 0.19$ and is in good agreement with data derived from the epoxy resin itself. At higher stress levels, the value of n increases due to microcracking within the composite. The largest difference in the creep-recovery behavior is exhibited between the first and second loading cycles, with n decreasing slightly with subsequent loading.

Nomenclature

c	= distance from beam neutral axis to outer fibers
D	= isotropic creep compliance
$D(t)$	= time-dependent isotropic creep compliance
D_0	= initial elastic compliance
D_1	= creep coefficient
ΔD	= net creep compliance, $D(t) - D_0 = D_1 t^n$
E_{11}	= longitudinal modulus
E_{22}	= transverse modulus
G_{12}	= shear modulus
$H(t)$	= Heaviside unit step function
I	= beam cross section moment of inertia about neutral axis
M	= applied moment
n	= creep exponent, $0 < n < 0.5$
$S_{11}, S_{22}, S_{12}, S_{66}$	= principal composite creep compliances in fiber coordinate system; 1, fiber direction, 2, normal to fiber direction
$S'_{11}, S'_{12}, S'_{22}, S'_{66}, S'_{16}, S'_{26}$	= transformed composite creep compliances in x-y coordinate system
$S'_{11}(t)$	= time-dependent composite creep compliance
S_0	= initial composite creep compliance, $S_{11}(0)$
S_1	= creep coefficient
$\Delta S'_{11}$	= net creep compliance, $S_1 t^n$
t	= time
ϵ	= strain
$\epsilon(t)$	= time-dependent strain
$\epsilon_1, \epsilon_2, \gamma_{12}$	= strains in fiber direction, normal to fiber direction, and shear strain, respectively
$\epsilon_x, \epsilon_y, \gamma_{xy}$	= strains transformed to arbitrary x-y axis
ν_{12}, ν_{21}	= major and minor Poisson's ratio, respectively
σ	= applied stress
σ_0	= applied creep stress (constant)
$\sigma_1, \sigma_2, \tau_{12}$	= stresses in fiber direction, normal to fiber direction, and shear stress, respectively
$\sigma_x, \sigma_y, \tau_{xy}$	= stresses transformed to arbitrary x-y axis
τ	= dummy time variable
$\theta, \pm\theta$	= fiber angle (unidirectional, angle ply)

Submitted June 8, 1982; presented as Paper 82-1068 at the AIAA/SAE/ASME 18th Joint Propulsion Conference, Cleveland, Ohio, June 21-23, 1982; revision received Aug. 11, 1983.

*Technical Specialist, Aerospace Division. Associate Fellow AIAA.

Introduction

FIBROUS composites have been used in several typical pressure vessels through the process of filament winding techniques. Fiber-reinforced epoxy composites are used in many solid propellant rocket motor cases to provide high strength and stiffness coupled with light weight. The case design involves a detailed consideration of the operational loads and environments sufficient to survive a specified service life period. Part of the motor case design depends upon a complete mechanical characterization of the case material and the subsequent application of these materials after the vessel has been subjected to one or more cycles of "hydrotesting" to pressure levels about 10–25% above the expected operating conditions. This technique of nondestructive testing (NDT) has, in fact, been shown to cause considerable internal damage to the composite, and in glass/epoxy composites, creates a condition for further damage due to moisture.[1,2] The hydrotest cycles tend to create microcracks, or crazing, at levels often as low as 40% of the burst pressure. This effect first was reported by Rawe,[3] in which he noted that the number of cracks was found to increase with pressurization and became a permanent feature of the case appearance upon release of the pressure. He also noted that a disproportionate amount of cracking occurred during the first (hydrotest) cycle. Crownover[1] suggests that a pressure level of 80% of the burst pressure causes a significant degree of damage or softening in the case material. His results showed that the strength reduction was a function of both the pressure level and the duration of the pressurization period. Although his observations were qualitative, they are consistent with the use of Lebesgue norms to describe the time-dependent crack growth effects, as originally suggested by Schapery et al.[4,5]

In addition to the hydrotest and final pressure loading cycles, the motor case also is subjected to a range of thermal environments. The majority of large solid rocket motors cur-

rently are designed to withstand a moderate temperature environment from 65 to 95°F. However, because more recent applications have broadened the temperature range, large ballistic missiles with composite cases operate in a 20–100°F environment. Air-launched and tactical motor cases are being developed to operate at temperatures specified within a −65–165°F envelope. Considering that normal cure conditions for most solid propellants are around 120–140°F, depending on propellant type and contractor facilities, the nominal operational temperature range for most large solid rocket motor cases is, therefore, about 20–140°F.

Many of these motor cases are subjected to internal pressurization during cure of the propellant at an elevated temperature for approximately 5–7 days. Pressure levels of 200–350 psig are often maintained during the cure cycle. These pressures are relatively low when compared to operational levels, being only about 10–30%. However, the pressure is applied continuously at moderately elevated temperatures, as noted previously. Earlier micromechanics modeling work by Beckwith[6,7] showed that even low stress level tests at 140°F resulted in a significant deviation from linear viscoelasticity theory as a result of internal crack growth and subsequent softening of the overall composite. Consequently, elevated temperature characterization of fiber-reinforced composites is important because linear theory does not always provide reliable engineering design properties through normal extrapolation procedures. Recent work by Beckwith[8] presented an approach for characterizing the nonlinear behavior of S-901 glass/epoxy laminates using Lebesgue norms to model multiple cycling effects such as exhibited during hydrotest and ignition loading. All previously reported work was essentially on autoclaved, flat-plate resin and laminate samples, whereas the current paper investigates the behavior of composite samples taken directly from a filament-wound motor case.

Theoretical Background

Viscoelastic behavior and constitutive theory for fiber-reinforced composite materials recently have been reviewed in detail by Schapery[9] and Beckwith.[10] No attempt will be made in this paper to go into the same depth, as only the necessary essentials will be reviewed and presented.

Matrix Viscoelastic Behavior and Constitutive Theory

Typical polymeric matrix materials fall into several classes of epoxies, phenolics, polyesters, etc., depending on the specific strength characteristics desired and many other design considerations. All of the materials exhibit some degree of viscoelasticity and generally are considered to be of a homogeneous, isotropic nature. The constitutive equation for a linear, viscoelastic polymeric matrix is given by the Boltzmann superposition integral for isothermal conditions as

$$\epsilon = \int_0^t D(t-\tau)\frac{d\sigma}{d\tau}d\tau \tag{1}$$

In the case of a uniaxial creep test the stress history is given by

$$\sigma = \sigma_0 H(t) \tag{2}$$

The resulting constitutive equation (1) then becomes

$$\epsilon(t) = D(t)\sigma_0 \tag{3}$$

The form of the creep compliance, $D(t)$, which has been found to represent the behavior of many rigid plastics both with and without reinforcement[11-14] is the power law form given by

$$D(t) = D_0 + D_1 t^n \tag{4}$$

where D_0, D_1, and n are positive constants which are independent of time. D_0 is the initial value of the creep compliance, D_1 the creep coefficient, and n is typically found to be $0 < n < 0.5$.

Lamina Constitutive Theory

To study the behavior of laminated fiber-reinforced composites, it is first necessary to establish the constitutive theory for the lamina (or laminae) using linear, elastic, anisotropic theory.[15,16] Fibrous composites generally are used in a manner such that the stress state is essentially two-dimensional and the assumptions of plane stress are invoked. Many composite materials also are treated as exhibiting transverse isotropy so that the constitutive equation may be written as

$$\begin{bmatrix}\epsilon_1\\ \epsilon_2\\ \gamma_{12}\end{bmatrix} = \begin{bmatrix}S_{11} & S_{12} & 0\\ S_{12} & S_{22} & 0\\ 0 & 0 & S_{66}\end{bmatrix}\begin{bmatrix}\sigma_1\\ \sigma_2\\ \tau_{12}\end{bmatrix} \tag{5}$$

where the coordinate system has been aligned with the lamina principal axes (1, fiber direction; 2, normal to fiber direction). When the material axes are referred to any other direction (x, y), the constitutive relations must be transformed using tensor transformations, e.g., Ashton et al.,[16]

$$\begin{bmatrix}\epsilon_x\\ \epsilon_y\\ \gamma_{xy}\end{bmatrix} = \begin{bmatrix}S'_{11} & S'_{12} & S'_{16}\\ S'_{12} & S'_{22} & S'_{26}\\ S'_{16} & S'_{26} & S'_{66}\end{bmatrix}\begin{bmatrix}\sigma_x\\ \sigma_y\\ \tau_{xy}\end{bmatrix} \tag{6}$$

Engineering constants usually refer to Young's moduli, Poisson's ratios, and shear moduli, which can be measured from simple tests. The following relations between the components of the S_{ij} and engineering constants are given as

$$S_{11} = 1/E_{11}, \qquad S_{22} = 1/E_{22}$$
$$S_{12} = -\nu_{12}/E_{11} = -\nu_{21}/E_{22}, \qquad S_{66} = 1/G_{12} \tag{7}$$

The linear, viscoelastic behavior of the orthotropic lamina (or laminae) in a state of plane stress, viz., Eqs. (5) and (6), may be written in the same form as Eq. (1),

$$\epsilon_1 = \int_0^t S_{11}(t-\tau)\frac{d\sigma_1}{d\tau}d\tau + \int_0^t S_{12}(t-\tau)\frac{d\sigma_2}{d\tau}d\tau$$
$$\epsilon_2 = \int_0^t S_{12}(t-\tau)\frac{d\sigma_1}{d\tau}d\tau + \int_0^t S_{22}(t-\tau)\frac{d\sigma_2}{d\tau}d\tau$$
$$\gamma_{12} = \int_0^t S_{66}(t-\tau)\frac{d\tau_{12}}{d\tau}d\tau \tag{8}$$

Similar expressions can be written for the constitutive equations in the transformed coordinate system. If the stress input is given as $\sigma_x = \sigma_0 H(t)$, i.e., a creep test for a uniaxial tensile specimen, then we obtain

$$\epsilon(t) = S'_{11}(t)\sigma_0 \tag{9}$$

where S'_{11} is used since the more general, transformed axes system for arbitrary fiber angle θ is chosen. In the case of off-angle tensile specimens, i.e., 0 deg $< \theta <$ 90 deg, the measured creep compliance is actually $S'_{11}(t)$. For $\theta = 0$ and 90 deg, S_{11} and S_{22} are measured for the respective angles directly. The form of the creep compliance corresponding to the matrix power law representation can be written as

$$S'_{11}(t) = S_0 + S_1 t^n \tag{10a}$$

where

$$S_0 = S'_{11}(0) \tag{10b}$$

Experimental Program

Resin and Laminated Plates

The experimental program was designed to provide the necessary isothermal data required to evaluate the effective (overall) laminate stiffness of a typical glass/epoxy composite material. The materials tested were representative of both the constituent materials as well as glass/epoxy composites used in a typical solid rocket motor case.

Tensile creep and recovery tests were conducted on Shell 58-68R epoxy resin, and laminates from the Shell 58-68R epoxy resin and S-901 glass. Both unidirectional and balanced ply laminates were constructed and tested. The materials were fabricated for the experimental program and made according to specifications used for typical solid rocket motor cases. Complete details concerning material and sample preparation are described in Ref. 10.

Tensile coupons with nominal 6-$\times\frac{1}{2}$-$\times\frac{1}{8}$-in. dimensions were fabricated from the various materials. Aluminum end tabs with $\frac{1}{8}$-in.-diam holes were used to load the samples on the creep machines. Strain gages were bonded to both sides of the sample to average out any induced bending effects. Localized heating effects were reduced by using 350Ω gages.

To characterize the epoxy resin and glass/epoxy composite, both single and multiple cycle creep and recovery tests were conducted. The creep tests consisted of rapidly applying a constant uniaxial load to the tensile coupon and measuring the resultant strain for a 1-h period. This test was followed immediately by a recovery test where the constant load was suddenly removed and the strain was measured for 2 h. The effects of multiple cycling were investigated for approximately three creep-recovery cycles to model typical hydrotest damage in filament-wound motor cases.

After completion of one cycle (creep-recovery), the total strain was recorded, the strain electrically rezeroed, and the next cycle initiated. The strain was therefore referred to the specimen length which existed at the end of each cycle. Tests on the Shell 58-68R epoxy resin matrix material were conducted over a temperature range of 20 to 160°F for two cycles of creep and recovery. Most of the creep and recovery tests carried out on the S-901 glass/Shell 58-68R epoxy resin were performed at 75 and 140°F with the exception of a few tests conducted on 45 and ±45 deg fiber angle glass/epoxy specimens at 20°F. As many as five different stress levels were studied for each fiber angle, depending on the degree of nonlinearity observed in the stress-strain curves.

The results of the epoxy resin tests clearly showed that the resin obeyed the power law creep compliance [Eq. (4)]. Figure 1 shows the net creep compliance [$\Delta D = D(t) - D_0 = D_1 t^n$] on a log–log plot, where the slope has a value of $n = 0.19$ over a wide temperature range from 20 to 160°F. Table 1 summarizes the power law constants (D_0, D_1) from both the creep and recovery portions of the tests. It was noted[6-8,10] that D_0 exhibited a temperature dependence as shown in Table 1.

For future reference purposes the linear viscoelastic creep compliances for the S-901 glass/epoxy composite are given in Table 2 for the unidirectional (θ) and angle-ply ($\pm\theta$) composite tests. All of the creep-recovery tests in the linear range exhibited an n value corresponding to the epoxy resin of 0.19 as predicted by micromechanics theory. Multiple cycle and high stress level tests at 140°F on the S-901 glass/epoxy composite showed considerable nonlinearity, as seen in Table 3. The value of n was typically quite high for the first cycle and then decreased with subsequent cycles. These results will be used later to compare with actual motor case results.

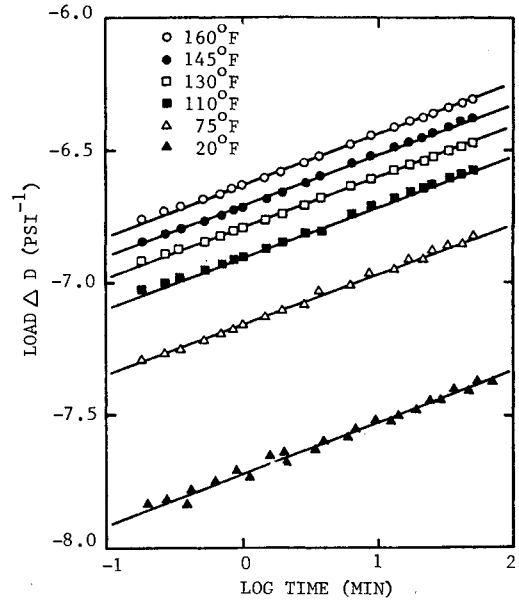

Fig. 1 Net creep compliance for Shell 58-68R epoxy.

Table 1 Power law constants for Shell 58-68R epoxy

Temperature, °F	$D_0 \times 10^{-6}$, psi^{-1}	$D_1 \times 10^{-6}$, from creep data	$D_1 \times 10^{-6}$, from recovery data
20	1.726	0.019	0.025
75	1.883	0.069	0.069
110	1.934	0.124	0.142
130	2.022	0.161	0.171
145	2.012	0.198	0.201
160	2.070	0.232	0.247

Table 2 Linear viscoelastic creep compliances for S-901 glass/epoxy

Temperature, °F	Fiber angle, deg	Creep compliance, S'_{l1}, $\times 10^{-6}$ (psi^{-1})
20	0	$0.1210 + 0.0003t^{0.19}$
	45	$0.3021 + 0.0046t^{0.19}$
	90	$0.3115 + 0.0025t^{0.19}$
	±45	$0.2876 + 0.0023t^{0.19}$
75	0	$0.1213 + 0.0004t^{0.19}$
	20	$0.1990 + 0.0038t^{0.19}$
	45	$0.3260 + 0.0124t^{0.19}$
	90	$0.3315 + 0.0081t^{0.19}$
	0/90	$0.1793 + 0.0015t^{0.19}$
	±30	$0.2037 + 0.0037t^{0.19}$
	±45	$0.3061 + 0.0082t^{0.19}$
	±60	$0.3534 + 0.0103t^{0.19}$
	±80	$0.3416 + 0.0152t^{0.19}$
140	0	$0.1265 + 0.0003t^{0.19}$
	20	$0.1957 + 0.0439t^{0.19}$
	45	$0.3524 + 0.0503t^{0.19}$
	90	$0.3490 + 0.1468t^{0.19}$
	0/90	$0.1829 + 0.0096t^{0.19}$
	±30	$0.2042 + 0.0345t^{0.19}$
	±45	$0.1881 + 0.3032t^{0.19}$
	±60	$0.3181 + 0.1786t^{0.19}$

Filament-Wound Motor Case Samples

To compare the effective stiffness of the composite plates with an actual motor case, a full-scale solid rocket motor case was used to obtain case specimens. Although the effects of the hydrotest damage may be significant with regard to the first loading cycle, the results of subsequent loading cycles (second through nth cycle) could be compared directly with the fabricated glass/epoxy plates. For this series of tests, the forward dome was chosen because the aft end has an outer layer of cork insulation which could not be removed easily without damaging the case material.

Samples were obtained from an area between two of the thrust termination ports. In this region, the motor case does

Table 3 Nonlinear creep compliances for S-901 glass/epoxy composite (140°F)

Fiber angle, deg	Stress, psi	Load cycle	Creep compliance, S'_{11}, $\times 10^{-6}$ (psi^{-1})
20	4,800	1	$0.2185 + 0.0097t^{0.41}$
		2	$0.2406 + 0.0105t^{0.39}$
		3	$0.2531 + 0.0123t^{0.35}$
20	8,500	1	$0.2633 + 0.0582t^{0.59}$
		2	$0.7196 + 0.0944t^{0.47}$
20	10,500	1	$0.2642 + 0.0555t^{0.59}$
		2	$0.7422 + 0.0873t^{0.45}$
45	3,000	1	$0.4102 + 0.1077t^{0.41}$
		2	$0.6947 + 0.0879t^{0.35}$
45	5,000	1	$0.4419 + 0.0221t^{0.53}$
		2	$0.4997 + 0.0602t^{0.27}$
		3	$0.5349 + 0.0722t^{0.23}$
45	6,500	1	$0.5264 + 0.1441t^{0.57}$
90	1,480	1	$0.4357 + 0.0498t^{0.45}$
		2	$0.5318 + 0.0649t^{0.35}$

not possess midplane symmetry because there are eight alternating layers. The fiber angles of samples taken from the meridional and circumferential directions were approximately ± 20 and ± 70 deg, respectively.

Several types of tests were conducted on these specimens. Direct comparison was to be made primarily using tensile creep-recovery tests in a manner similar to the resin and laminated plate coupons. Four-point beam bending tests were conducted using two different loading modes: creep-recovery and constant displacement rate conditions. The ± 70-deg samples were tested in tension because of the lower degree of curvature. Stress levels of 300 and 1000 psi were used for these tests for three creep and recovery cycles. The four-point beam bending tests gave a constant moment between the two center loading points. Both ± 20- and ± 70-deg samples were used at at least two bending moments. The constant displacement rate conditions were applied to the center loading points and the strain gage and crosshead displacement monitored throughout the load cycle. Two or three load-unload cycles were made on each sample. All tests were conducted at 75°F and ambient humidity (about 30% relative humidity). The fiber volume on the autoclaved plates averaged 0.616, whereas the volume fiber in the motor case samples was found to be 0.635.

Filament-Wound Case Results

The tensile creep-recovery tests on the ± 70-deg fiber angle case samples were conducted for two nominal stress levels, 300 and 1000 psi. Figures 2 and 3 show the effects of both stress level and multiple cycling. Remember that these materials have already been stressed to a high level during the actual motor case hydroproof. Although the case was not burst, some damage was evident in the dome region through the appearance of microcracking, or crazing. However, several observations can be made at this point. The first is that the higher stress level (1000 psi) is softer and apparently reflects some internal damage. The second observation is that there is a disproportionate amount of change between the first and second creep-recovery cycles. This was also noticed in the laminated plates, and was a particularly strong effect in ± 45-, ± 60-, and ± 80-deg angle-ply samples at even moderate stress levels.[7,8,10] Lou and Schapery[17] found that as many as 5–10 creep-recovery cycles were required to stabilize E-glass/epoxy unidirectional composites at elevated temperatures.

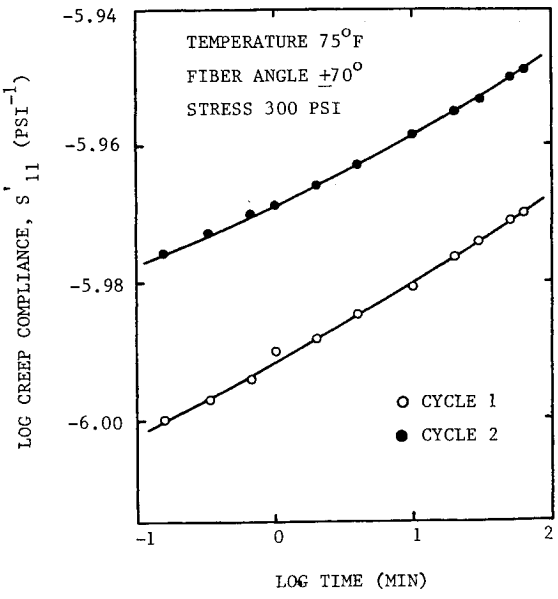

Fig. 2 Effect of multiple loading on creep compliance (300 psi stress).

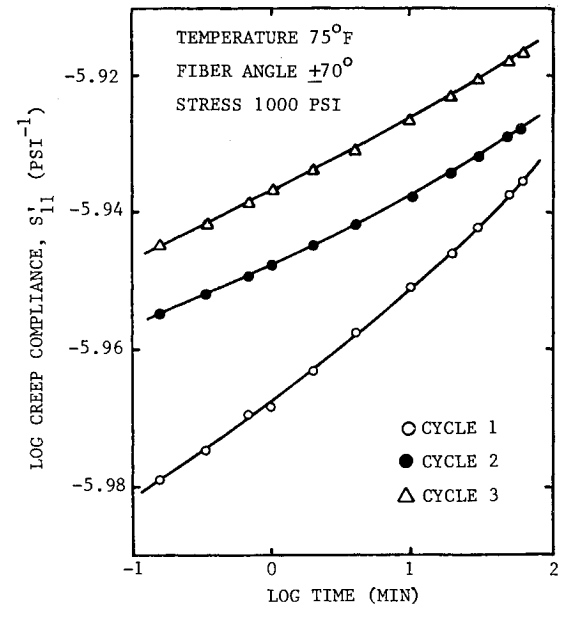

Fig. 3 Effect of multiple loading on creep compliance (1000 psi stress).

The net creep compliance, $\Delta S'_{11}$ or $S_1 t^n$, was plotted on a log–log scale as shown in Figs. 4 and 5 after assuming $n = 0.19$ and determining the best fit values for S_0 and S_1. The slope of the curves is indeed 0.19, with excellent agreement with both the earlier resin data as well as the laminated (autoclaved) plate data. It can also be seen that the value of S_1 decreases slightly with each successive cycle of creep and recovery. The effect again is more pronounced with the higher stress levels. Looking at Table 3 it can be seen that there are significant changes between the first and second creep-recovery cycles for the laminated plates and much less between subsequent cycles. Also, it is of interest to note that the value of S_1 generally increases for the laminated plate results, whereas the ± 70-deg test results show a decrease. The changes in the laminated plate also were found to be more severe (50% between first and second cycles and 10–20% between second and third cycles, on the average) than that seen in the case materials. It is believed that the ± 70-deg orientation has already experienced significant nonlinear damage due to the hydroproof tests. Consequently, one should not expect as good a correlation in the absence of first cycle data.

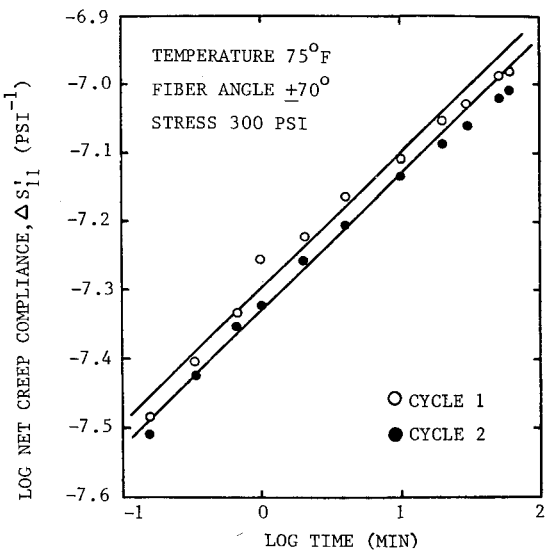

Fig. 4 Net creep compliance for case material (300 psi stress).

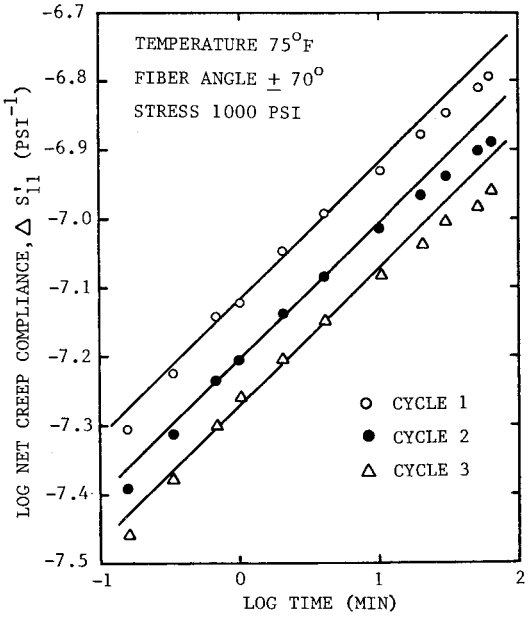

Fig. 5 Net creep compliance for case material (1000 psi stress).

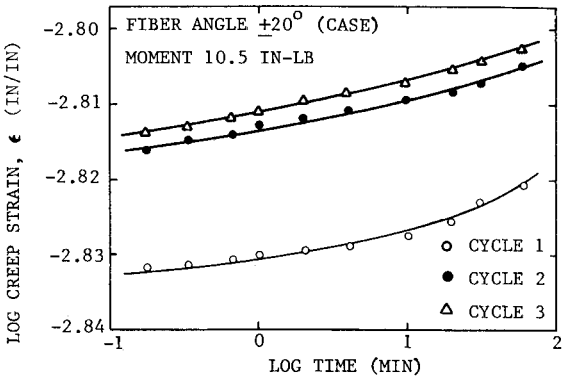

Fig. 6 Effect of multiple cycling for ±20-deg case material beam.

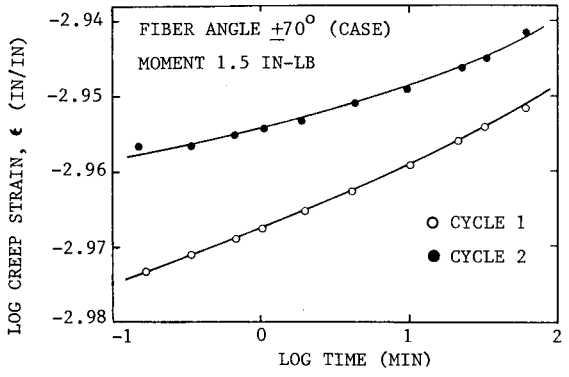

Fig. 7 Effect of multiple cycling for ±70-deg case material beam (1.5 in.-lb moment).

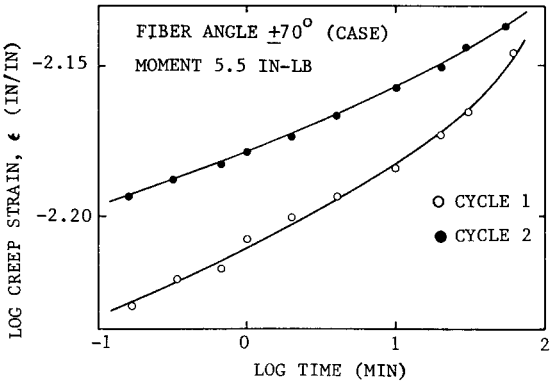

Fig. 8 Effect of multiple cycling for ±70-deg case material beam (5.5 in.-lb moment).

The previously described uniaxial tensile tests were conducted to investigate the time and temperature dependence of the S-901 glass/epoxy composites.[10] The studies have shown that the glass/epoxy materials are nonlinearly viscoelastic,[6,7,10] probably due in part to the time-dependent development and growth of microscopic cracks. The degree of nonlinearity depends on many factors which have been cited already; namely, stress level, temperature, fiber angle, etc. However, the uniaxial tensile test differs significantly from a bending test in that a strain gradient exists across the thickness which is not present in the former one (neglecting a slight amount of bending due to grip effects). This series of tests was conducted to determine the effect of the strain gradient on material nonlinearity.

The results from some of the creep and recovery tests are shown in Figs. 6–8. The data are plotted as usual for the previous tests of this type, except that strain ϵ rather than compliance is used. Strictly speaking, we cannot assume that all of the layers of the beam are within the linear viscoelastic range, particularly in the presence of a significant strain gradient. Neglecting this situation for the moment, we shall study some of the behavior shown by the beam tests. Remember also that the strain used here represents the output from the strain gage on the tension side of the beam.

In general, the beam cycle-to-cycle variation behaves in the same manner as the tensile coupons, showing a disproportionate change between the first and second loading cycles. It has been found that the strain can be represented by the power law in time with $n = 0.19$ for all the tests, regardless of fiber angle or stress level, with excellent correlation at each cycle.

With the behavior pattern now established, let us assume that the stress σ at the outer fibers of the beam is still within the linear range. Consequently, we can use the flexure formula

$$\sigma = Mc/I \tag{11}$$

Linear elastic (viscoelastic) behavior was assumed, although at the higher stress levels this will not be true. The creep compliance may be determined in the same manner as in the previous tests for the constant applied stress. Table 4 shows the

Table 4 Beam creep and recovery compliances

Fiber angle, deg	Moment, in.-lb	Load cycle	Compliance, $\times 10^{-6}$ (psi^{-1})
±45	12.5	1	$0.3000 + 0.0083t^{0.19}$
		2	$0.3027 + 0.0085t^{0.19}$
±45	55.5	1	$0.3980 + 0.0097t^{0.19}$
		2	$0.4205 + 0.0067t^{0.19}$
		3	$0.4371 + 0.0032t^{0.19}$
±20 case	10.5	1	$0.1657 + 0.0024t^{0.19}$
		2	$0.1724 + 0.0025t^{0.19}$
		3	$0.1735 + 0.0028t^{0.19}$
±70 case	1.5	1	$0.7694 + 0.0291t^{0.19}$
		2	$0.7753 + 0.0295t^{0.19}$
		3	$0.8085 + 0.0212t^{0.19}$
±70 case	5.5	1	$1.5060 + 0.1899t^{0.19}$
		2	$1.6394 + 0.1758t^{0.19}$

effective creep compliance found by using the stress defined by Eq. (11).

The initial creep compliance for the ±45-deg S-901 glass/epoxy tested at the bending moment of 12.5 in.-lb is within 2% of the value shown in Table 2 for the uniaxial tensile creep and recovery tests. The creep coefficient, which does not change significantly with subsequent cycles, also agrees with the uniaxial data. At the higher stress levels (moments) the ±45-deg S-901 glass/epoxy exhibits the softening effect seen in the tensile coupons.

Consider the ±20-deg S-901 glass/epoxy case material next. In earlier works[6,10] the angular dependence of the linear viscoelastic creep compliances was predicted. From the predicted curve based on third cycle data the initial compliance was found to be 0.187×10^{-6} (psi^{-1}), which agrees reasonably well with the beam values. The agreement is within 4.5% after correcting for the difference in the fiber volume fraction using the actual motor case data. The third cycle beam data were corrected by simply multiplying by the ratio of the fiber volume fractions, i.e., 0.635/0.616, to obtain an estimated initial creep compliance.

The ±70-deg case material does not show good agreement with the initial linear creep compliance of 0.348×10^{-6} (psi^{-1}) which would be predicted,[6,10] being in error by about 100%. However, the strain which exists at the outer fibers of the beam is on the same order of magnitude as the earlier tensile creep and recovery tests which had also indicated significant softening. It is not unreasonable to expect severe softening after one considers the prior history of the case as a result of hydrotesting. There is a considerable number of surface cracks present in the case materials as a result of the earlier hydrotesting. The material is, therefore, much softer in the dome region of the motor case, where the fiber angles are greater (near ±70 deg), than in the cylinder section (0/90 deg).

Another interesting feature is the relative growth in the initial creep compliance for the ±70-deg S-901 glass/epoxy with each cycle, while the creep coefficient remains virtually unchanged from cycle to cycle. The normal stress is considerably higher than the shear stress for the ±70-deg fiber angle and would tend to explain this behavior in terms of sudden (rather than slow) crack growth.

The constant displacement rate tests were conducted to study the effects of multiple cycling under controlled displacement conditions. The test has been observed to be essentially a constant strain rate test for the sample stiffnesses encountered. The effects of multiple cycles are shown in Figs. 9 and 10 for fiber angles of ±20 and ±70 deg in the motor case samples.

The cyclic loading of the motor case materials appears to have reached an equilibrium behavior. The hysteresis loop remains essentially unchanged from cycle to cycle except at the higher moments. The material exhibits considerable softening in the initial compliance (Table 4), although the creep coefficient which reflects time-dependent crack growth appears to remain unchanged with successive cycles. The ±20-deg fiber angle specimens agree well with linear theory at low stress levels (< 5 in.-lb) and show little hysteresis. However, the ±70-deg samples, as previously noted, exhibit considerable softening and do not agree at all with linear beam theory.

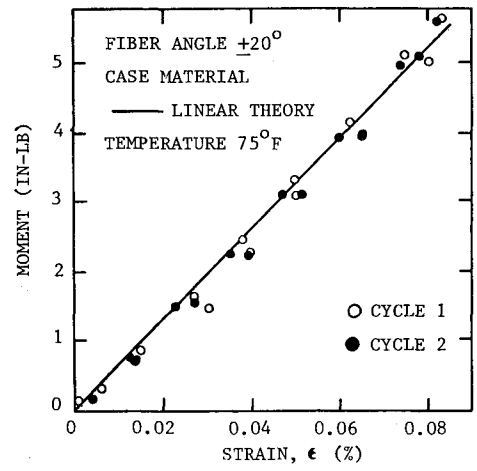

Fig. 9 Effect of cyclic loading of ±20-deg beam (case material).

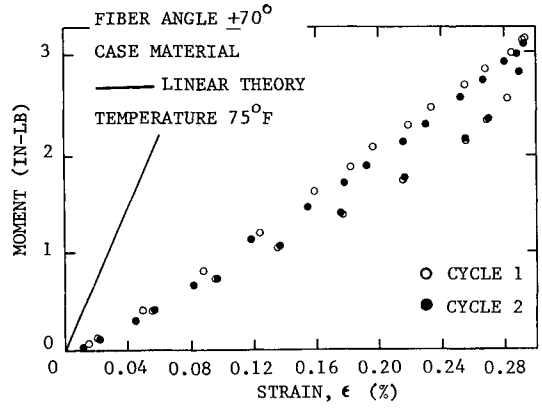

Fig. 10 Effect of cyclic loading of ±70-deg beam (case material).

Conclusions

Many of the characteristics seen in the earlier resin and laminated (autoclaved) plate tests on the S-901 glass/epoxy are also seen in the filament-wound motor case specimens. They both appear to obey micromechanics theory in the linear viscoelastic region, reflecting an n value of 0.19 as seen in the resin. The ±20-deg fiber angle samples, having seen predominantly lower stresses during hydrotest, agree well with the laminated plate results and linear theory. The ±70-deg fiber angle materials exhibit a large departure from linear theory, most likely due to the presence of microcracking and resin crazing.

As in the laminated plate tests, the most significant difference in creep behavior is exhibited between the first and second loading cycles, whether the loading is in tension or bending. The changes with each cycle are more apparent in tension loading (Table 3) than in bending (Table 4), where crack arrest appears to be taking place. The presence of a strong strain gradient in the beam tests can provide a significant mechanism for crack arrest between layers (plies).

Acknowledgments

The work was funded under Contract F04611-72-C-0055 with the Air Force Rocket Propulsion Laboratory (Air Force Systems Command) as part of a study to evaluate the nonlinear, viscoelastic behavior of S-901 glass/epoxy composite materials.

References

[1]Crownover, W.S., "Demonstration of High Strength Fiberglass Reinforced Composite Motor Case Technology," RK-TR-69-5, Army Propulsion Laboratory and Center, Redstone Arsenal, Alabama, April 1969.

[2]Jensen, W.M., Knoell, A.C., and Zweben, C., "Development of Boron/Epoxy Rocket Motor Chambers," *Proceedings of the 27th Annual Technical Conference, Society of the Plastics Industry, Inc.*, 1972, p. 17-C-1.

[3]Rawe, R.A., "Craze Cracking in Glass Filament-Wound Pressure Chambers," *Symposium on Standards for Filament-Wound Reinforced Plastics*, ASTM STP-327, 1963, p. 248.

[4]Schapery, R.A., Beckwith, S.W., and Conrad, N., "Studies on the Viscoelastic Behavior of Fiber-Reinforced Plastic," AFML-TR-73-179, July 1973.

[5]Farris, R.J. and Schapery, R.A., "Development of a Solid Rocket Propellant Nonlinear Viscoelastic Constitutive Theory," AFRPL-TR-73-50, June 1973.

[6]Beckwith, S.W., "Viscoelastic Characterization of a Nonlinear, Glass/Epoxy Composite Using Micromechanics Theory," *JANNAF Operational Serviceability and Structures and Mechanical Behavior Working Groups*, Feb. 1975, CPIA Pub. 264, May 1975, p. 271.

[7]Beckwith, S.W., "Creep Evaluation of a Glass/Epoxy Composite," *Proceedings of the 11th National SAMPE Technical Conference*, Nov. 1979, p. 513; also, *SAMPE Quarterly*, Vol. 11, Jan. 1980, p. 8.

[8]Beckwith, S.W., "Nonlinear Viscoelastic Characterization of a Composite Case Material at Operational Temperatures," *JANNAF Structures and Mechanical Behavior Working Group (1980 Meeting)*, Oct. 1980, CPIA Pub. 331, Jan. 1981, p. 163.

[9]Schapery, R.A., "Viscoelastic Behavior and Analysis of Composite Materials," Mechanics and Materials Research Center, Texas A&M University, College Station, Tex., Tech. Rept. MM-72-3, Aug. 1972.

[10]Beckwith, S.W., "Viscoelastic Characterization of a Nonlinear, Glass/Epoxy Composite Including the Effects of Damage," Ph.D. Dissertation, Mechanics and Materials Research Center, Texas A&M University, College Station, Tex., Tech. Rept. 2895-74-8, Oct. 1974.

[11]McCammond, D., "The Substitution of Time-Dependent Data in Hookean Formulae," *Transactions of Journal of Plastics Institute*, Vol. 35, 1967, p. 409.

[12]Ward, I.M., *Mechanical Properties of Solid Polymers*, Wiley Interscience, New York, 1971.

[13]Findley, W.N., "Creep Characteristics of Plastics," *American Society of Testing Materials, Symposium on Plastics*, 1944, p. 118.

[14]Thorkildsen, R.L., "Mechanical Behavior," *Engineering Design for Plastics*, edited by E. Baer, Reinhold Publishing Corp., Florence, Ky., 1964, p. 277.

[15]Lekhnitskii, S.G., *Theory of Elasticity of an Anisotropic Body*, translated from the Russian by P. Fern, edited by J. Brandstatter, Holden-Day, Oakland, Calif., 1963.

[16]Ashton, J.E., Halpin, J.C., and Petit, P.H., *Primer on Composite Materials: Analysis*, Technomic Publishing Co., Inc., Lancaster, Pa., 1969.

[17]Lou, Y.C. and Schapery, R.A., "Viscoelastic Characterization of a Nonlinear Fiber-Reinforced Plastic," *Journal of Composite Materials*, Vol. 5, April 1971, p. 208.